

Circular dichroism: A powerful tool for studying biomineralization promoter proteins

Melika Sarem and Steffen Lüdeke

Biomineralization is the matrix-directed calcification of tissue in living organisms. The deposition of different polymorphs of calcium phosphate or calcium carbonate is a highly regulated process. It may involve cell-controlled mechanisms with vesicular delivery of inorganic material to the extracellular matrix and cell-independent processes mediated by dedicated matrix proteins. These proteins promote the formation of microscopic crystals of defined size and shape, which combine to form bio-inorganic materials with unique properties. Successful biomineralization is correlated with structural elements, such as matrix proteins involved in the nucleation process. Circular dichroism (CD) is a spectroscopic technique for the determination of a secondary structure of proteins and has therefore been applied for studying numerous biomineralization promoter proteins. This article reviews and compares CD data on matrix proteins from different contexts, such as eggs, seashells, and teeth. It highlights the potential of CD for secondary structure determination and quantification and points out pitfalls that may lead to misinterpretation of CD spectra. The data suggest that most biomineralization promoter proteins contain domains of different secondary structure with predominantly unordered conformation. However, they may acquire a higher degree of order initiated by environmental factors such as pH, presence of cations, or charged surfaces.

Introduction

Mineralized tissue, such as eggshells, mollusk shells, teeth, or bone, forms through highly regulated deposition of inorganic material on an organic matrix. The minerals involved in biomineralization are mostly precipitates of calcium phosphate and calcium carbonate. They appear as different crystal modifications in different tissues, such as hydroxylapatite ($Ca_{10}(PO_4)_6(OH)_2$) in teeth and bone, or calcite, aragonite, or vaterite (different polymorphs of $CaCO_3$) in mollusk shells or eggshells.

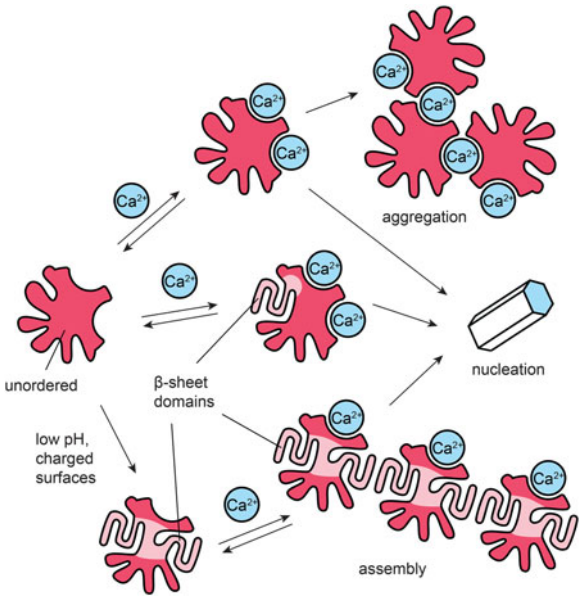
As both hypo- and hypermineralization result in non-viable materials, biomineralization has to provide very distinct arrangements of crystallites. This happens through a precise mechanism, which may be either cell-controlled or cell-independent.[1] In cell-controlled processes, ions or preformed precipitates of inorganic material are delivered in lipid vesicles to the extracellular space and released after subsequent rupture. In cell-independent processes, minerals form on biological matrices with dedicated biomineralization promoter proteins (BPPs) as a template to trigger the nucleation of nanometer-sized crystals.[2,3] The modulation of BPP-mediated processes likely involves conformational changes that lead to a shift in secondary structure, the three-dimensional fold of the amino acid chain that constitutes the protein.

Various factors have an influence on the equilibrium between two or more conformations in cell-independent biomineralization (**Scheme 1**). It has been shown for various BPPs that they are intrinsically unordered and highly charged.[3] Therefore, it is not surprising that their conformation is sensitive to pH. Furthermore, as a mineral cation binds to charged domains of the active conformation of a BPP, it also stabilizes this conformation. Some proteins take up some degree of β-sheet secondary structure, a highly ordered protein fold in which aligned amino acid strands interact through hydrogen bonding. Some studies report aggregation of BPPs upon the addition of bivalent cations such as Ca^{2+}—this could either be mediated through ionic cross-linking or through β-sheet domains, which are generally known to have a propensity for driving

Melika Sarem, Institute for Macromolecular Chemistry, University of Freiburg; Helmholtz Virtual Institute on Multifunctional Biomaterials for Medicine, Kantstr. 55, 14513 Teltow, Germany; Bioss, Centre for Biological Signalling Studies, University of Freiburg, Germany; melika.sarem@makro.uni-freiburg.de
Steffen Lüdeke, Institute of Pharmaceutical Sciences, The University of Freiburg, Germany; steffen.luedeke@pharmazie.uni-freiburg.de
DOI: 10.1557/mrs.2015.116

© 2015 Materials Research Society

https://doi.org/10.1557/mrs.2015.116 Published online by Cambridge University Press



Scheme 1. Hypothetical structural prerequisites for protein-promoted nucleation. Conformational transitions may be driven by binding of bivalent cations and other environmental factors, such as pH or charged surfaces. Protein assembly/aggregation is frequently observed for biomineralization promoter proteins and may also be important for mineralization.[4–7]

protein or peptide assembly.[8] In a physiological environment, charge–charge interactions with BPPs may also happen at charged surfaces, such as scaffolding proteins or charged lipids. To understand this complicated interplay of factors, it is necessary to know the secondary structure of a promoter protein in the biomineralization process.

This article briefly introduces circular dichroism (CD) spectroscopy as a tool for the determination and quantification of a secondary structure of proteins and peptides in general and highlights its use for studies on BPPs in particular. It provides a comparison of CD spectra of a selection of BPPs from mineralized tissue in different species (avian eggshell, mollusk shell, mammalian tooth) and reveals striking similarities in spectral features and in the conformational behavior of these proteins toward environmental stimuli, such as pH, bivalent cations, or charged surfaces.

Circular dichroism: Principles

CD is a spectroscopic technique that is highly sensitive toward secondary structures. It has therefore been used in numerous studies to analyze the fold of biomineralization-associated proteins. A CD spectrometer generates circularly polarized radiation, which means that its electric field vector describes a helix along the axis of propagation (**Figure 1**a). The interaction with an asymmetric (chiral) molecule such as a protein is different, whether this helical radiation is left-handed (left circularly polarized light [CPL]) or right-handed (right CPL). Therefore, CD is defined as the difference in absorbance of left CPL and right CPL.

When ultraviolet light excites the electrons of carbonyl groups in the protein backbone, this gives rise to coupled transition dipole moments with a helical disposition.[9] The CD intensity that corresponds to these coupled π–π* and n–π* transitions exceeds the signal intensities associated with the chiral centers of single amino acids by orders of magnitude. In different protein folds, the coupling of these transitions is also different, which results in characteristic CD patterns for secondary structures that are similar throughout most proteins and peptides. For a β-helix, there are usually a positive band at ~190 nm and two negative bands at ~207 nm and 222 nm. A β-sheet exhibits a positive band near 195 nm and a negative band at ~217 nm, and an unordered conformation has a strong negative band at ~197 nm and sometimes a weak positive band at ~220 nm (Figure 1b).[9] "Unordered" does not mean that a protein's fold is random, such as in synthetic polymers. It still has fixed positions and orientations of consecutive residues, although they may not necessarily be in continuous order.[15] For example, the positive shoulder at ~220 nm indicates a P_{II}-helix, a structural motif that is present in most unordered proteins.[16–18] Therefore, the widely used term "random coil" will be avoided and replaced by "unordered" throughout this article.

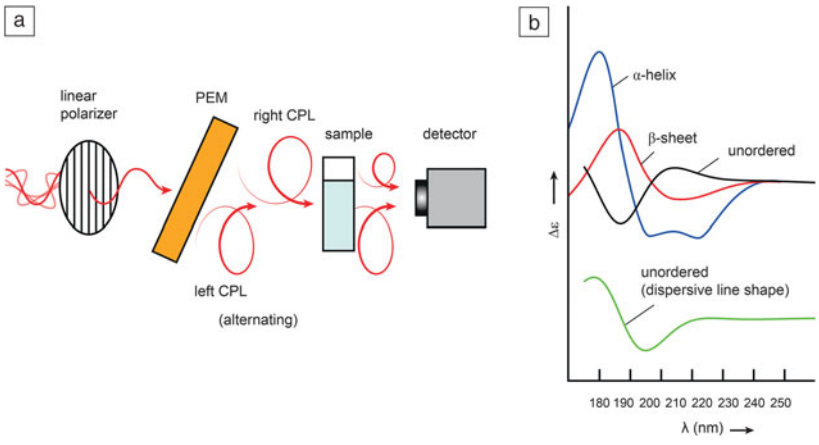


Figure 1. (a) Elements of a circular dichroism (CD) spectrometer. The photoelastic modulator (PEM) generates alternatingly left and right circularly polarized light (CPL). A chiral sample has different absorbance for left and right CPL (indicated by different amplitudes after passage through the sample). (b) Prototypic CD spectra for α-helix (poly-L-glutamic acid, pH 4.5, blue) (adapted with permission from Reference 10. © 1972 American Chemical Society). β-sheet (poly-L-lysine-L-leucine, 0.5 M NaF, pH 7, red (adapted with permission from Reference 11. © 1980 Elsevier). Unordered secondary structure (poly-L-lysine, pH 7, black) (recorded on a Jasco J-810 Spectropolarimeter). The black spectrum is in agreement with previously published CD spectra of poly-L-lysine[12,13] and has the typical curve shape of peptides with unordered conformation.[14] The dispersive curve of an unordered secondary structure (green), obtained from the Kramers–Kronig transform of the black spectrum, is offset for better comparison.

https://doi.org/10.1557/mrs.2015.116 Published online by Cambridge University Press

CD and biomineralization: Potential and challenges

A CD experiment can be performed on the timescale of minutes, and a secondary structure is assigned in a straightforward way by comparing the CD spectrum of the protein of interest to prototypic spectra as shown in Figure 1b. Other conformation sensitive methods, such as Fourier transform infrared spectroscopy, provide less characteristic spectra, and in the case of nuclear magnetic resonance (NMR), expensive isotopic labeling of recombinant proteins is a necessary first step. Since in biomineralization processes subtle shifts between conformations occur (Scheme 1), it is obvious that in this context, the quantification of proportions of secondary structure is at least as important as their qualitative assignment.

According to Beer's law, the CD spectrum represents a linear combination of the spectral contributions from all components present in the sample.[19] This is a major difference compared to NMR, where the spectra represent an ensemble average. CD-based secondary structure quantification can be performed either on the basis of representative CD-spectra of model peptides or for more accurate evaluation through multivariate methods. For the latter, spectral comparison software utilizes databases of protein CD spectra and provides as an output the percentage of α-helix, β-sheet, unordered conformation, and other structural elements that are present in the analyzed protein.[9,20,21] Furthermore, theoretical models for the quantum-chemical simulation of protein CD have recently been implemented in computer software.[22] As these tools are increasingly used to understand how spectral features are correlated with secondary structures, advances in computational methods will continue to contribute to the evolution, and sustained and successful use, of CD for protein analysis.

An underestimated problem in protein CD arises from scattering effects. Some studies on BPPs report aggregation and opaqueness of sample solutions under the conditions which the CD spectra were measured. However, an assignment based on prototypic spectra, as shown in Figure 1b, is restricted to proteins in the solution state. If the proteins of interest form suspended particles, they may cause differential scattering (instead of absorbance) of left and right circularly polarized light, which leads to spectra with dispersive line shape.[23] In this case, considerable spectral changes are observed, although the secondary structure of the monomeric molecule is more or less unchanged. In theory, the absorptive curve (CD spectrum) and the dispersive curve (differential scattering) are mathematically related by the Kramers–Kronig transform.[24] The theoretical dispersive spectrum of particles formed from proteins with unordered conformation is shown in Figure 1b. The superficial resemblance to the CD spectrum of the α-helix demonstrates that the presence of scattering protein aggregates may severely complicate the assignment and quantification of secondary structure. However, if taken into account, such spectral features may also serve as a probe for the assembly of proteins with still intact folds, which may play an important role in biomineralization.

Matrix proteins in avian eggs: Phosvitin and ovocleidin

Phosvitin is a very hydrophilic phosphoprotein that is highly abundant in the yolk of hen eggs.[25,26] Analogous to other nucleation-inducing proteins that are generally highly phosphorylated, phosvitin has been shown to promote the formation of minerals, such as calcium phosphate[27] and hydroxylapatite.[28,29] The physiological role of phosvitin is associated with skeletal development[30] rather than with the formation of hen eggshell. The deposition of calcite in the eggshell depends on a complex array of distinct proteins, in addition to ovocleidin-17, which is the most abundant protein found in hen eggshell extracts.[31]

Effect of pH

Among the various environmental variables, the pH of the biomineralization microenvironment is a particularly important one, as BPPs tend to be highly charged. With 110 phosphoserine residues that account for about 50% of its amino acids[26] and numerous aspartate and glutamate residues[32] phosvitin is an extraordinarily acidic protein. The pH-titration curve of phosvitin shows two equivalence points,[25,33] with pK_1 and pK_2 values of approximately 7.2 and 2.5.[34]

CD spectra recorded at different pH values show that these transitions are concomitant with a change in secondary structure (**Figure 2**).[34,35] At pH 6.6, the phosvitin spectrum exhibits a strong negative band at 198 nm, combined with a weak positive and a weak negative band at 219 nm and 232 nm, respectively. Such a band pattern is in perfect agreement with an unordered conformation. Lowering the pH to 3.4 does not lead to any substantial spectral changes, except for a lower intensity of the shoulder at 220 nm. As stated previously, a shoulder

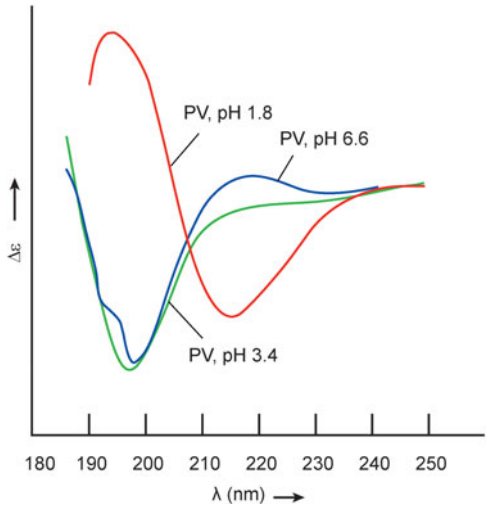


Figure 2. Circular dichroism spectra of phosvitin recorded at pH 6.6, pH 3.4, and pH 1.8. Phosvitin (PV) has unordered conformation in a broad pH range and adopts a β-sheet structure at low pH. pH 6.6 adapted with permission from Reference 35. pH 3.4 and pH 1.8 adapted with permission from Reference 34.

https://doi.org/10.1557/mrs.2015.116 Published online by Cambridge University Press

at 220 nm indicates the presence of a P_{II}-helix. The P_{II}-helix has originally been described as the left-handed helical form adopted by oligo-L-prolines in water.[36,37] However, this structural motif is present in a large number or even most unordered proteins and peptides and does not require the presence of a proline ring.[16–18,38,39] Therefore, the pH-dependent change in the intensity of the shoulder at 220 nm in the CD spectrum of phosvitin indicates a transition between two different unordered conformations around physiological pH. It is a well-known phenomenon that secondary structure may change due to removal of electrostatic repulsion through pH-dependent neutralization of charged residues, allowing for a more compact, higher-order conformation.[40] In agreement with this, the spectrum at pH 1.8 shows characteristic features (maximum at ~195 nm and minimum at ~220 nm) of a β-sheet.

Effect of interaction with cations

As the neutralization of negatively charged residues leads to conformational changes, a similar effect can be observed for phosvitin in the presence of cations. Effects of ionic strength[41] or Fe^{3+} ions[42] on phosvitin structures have been reported. In the context of biomineralization, the effects of the bivalent cations Ca^{2+} and Mg^{2+} are of particular interest. For different pH, conformational transitions of phosvitin were concomitant with changes in the CD intensity at 220 nm (see Figure 2). Interestingly, the addition of Ca^{2+} ions generates a negative shoulder between 220 nm and 230 nm in the CD spectrum, which indicates β-sheet formation. On the other hand, the addition of Mg^{2+} ions results in a positive CD signal around 220 nm,[43] a hallmark for unordered structure containing the P_{II}-helix (**Figure 3**a).[16–18] The presence of either Ca^{2+} or Mg^{2+} has an opposite effect on phosvitin conformation and suggests that the cation effect does not depend on charge neutralization alone. Not all charged groups are equally accessible for different cations. It has been assumed that this different selectivity for Ca^{2+} or Mg^{2+} leads to different conformations of the phosvitin/cation complex.[43]

The eggshell protein ovocleidin-17 also exhibits sensitivity toward addition of Ca^{2+} ions that is reflected by changes in the CD spectrum (Figure 3b).[44] In absence of Ca^{2+}, there is a minimum at 207 nm and a maximum below 195 nm that indicate the existence of domains with α-helical structure being in agreement with the crystal structure of ovocleidin-17.[45] However, because the α-helix spectrum has a much higher intensity than the spectra of other conformations, a CD spectrum might show the qualitative features of an α-helix, although it contains a significant amount of other secondary structures.[9] Indeed, the existence of a shoulder around 196 nm in the CD spectrum of ovocleidin-17 also indicates the presence of unordered conformation.[44] The addition of Ca^{2+} ions changes the curve shape and leads to a negative shoulder around 225 nm, which suggests some degree of β-sheet formation upon calcium binding. This would agree with the effect of Ca^{2+} binding to phosvitin, where the changes in the CD spectrum are consistent with a Ca^{2+}-induced conformational change (Figure 3a).[43]

Charge effects are not restricted to the influence of pH and the presence of inorganic cations. Biomineralization occurs at organic matrices that are very often charged. Given that the p*K* values of the lysine and arginine side chains are 10.67 and 12.10, respectively,[46] the polybases poly-L-lysine and arginine-rich protamine are generally charged at physiological (around neutral) pH and are therefore good models for organic polycationic materials. In the presence of poly-L-lysine or protamine, the CD spectrum of phosvitin has a β-sheet like appearance (Figure 3c).[47] As both poly-L-lysine and protamine

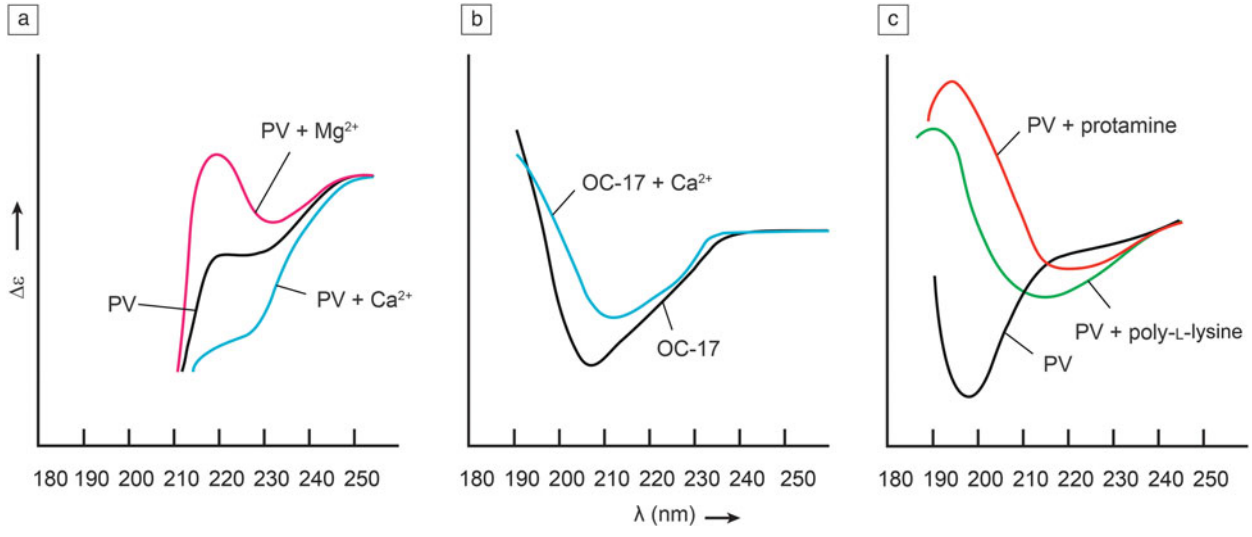


Figure 3. (a) Binding of bivalent cations to phosvitin (PV). (b) Ovocleidin-17 (OC-17) with and without Ca^{2+}. (c) Interaction of PV with poly-L-lysine and protamine. Interaction with positive charge invokes conformational changes in avian biomineralization promoter proteins. (a) Adapted with permission from Reference 43. (b) Adapted with permission from Reference 44. (c) Adapted with permission from Reference 47.

https://doi.org/10.1557/mrs.2015.116 Published online by Cambridge University Press

have unordered structure, this indicates a conformational change in phosvitin invoked by the presence of a polycation. Compared to the β-sheet spectrum obtained at low pH (Figure 2) in the CD spectrum of the complex of phosvitin and poly-L-lysine, the minimum is considerably broader, and both the maximum and minimum are blue shifted. As mixing of phosvitin with polycations leads to cloudiness of the sample solution,[47] there may also be spectral contributions from differential scattering arising from aggregated particles of unordered conformation, as demonstrated in Figure 1b.

Matrix proteins from mollusk shells

Some marine mollusks deposit different polymorphs of calcium carbonate in different layers of their shell, with the outer (prismatic) layer being formed out of calcite and the inner (nacreous) layer consisting of aragonite.[48] The growth of the shell occurs in the extrapallial (EP) fluid, a liquid medium that fills a thin cavity between the soft parts of the mollusk and the external shell. Whether calcite or aragonite is obtained during mineralization depends on the presence of magnesium ions. Low magnesium levels are incorporated into calcite, thereby making it less stable; in contrast, higher concentrations of magnesium induce the formation of aragonite.[49] The balance of Ca^{2+}/Mg^{2+} insertion is a highly regulated process that depends on mineralization inducing or inhibiting proteins that generally contain characteristic sequential motifs of acidic amino acid residues.[50–52]

Effect of interaction with cations

EP fluid protein is a glycoprotein that has been purified from EP extracts of the blue mussel (*Mytilus edulis*).[53] It contains an unusual pattern of histidine (His) and aspartate (Asp) amino acid residues that occur in pairs: Asp-Asp-His-His-Asp-Asp-His-His-Asp···His-His-Asp. The overall high content of acidic residues (25.15%) suggests a role as a BPP. The CD spectrum of the EP fluid protein recorded in absence of calcium clearly indicates unordered conformation (**Figure 4**a).[53] The CD spectrum in the presence of Ca^{2+} has been assigned to α-helical conformation, however electrophoresis and sedimentation analyses have also shown that the EP fluid protein forms protomeric assemblies in the presence of calcium.[53] Therefore, similar to phosvitin in presence of polycations (Figure 3c), the CD spectrum may as well contain contributions from differential scattering (Figure 1b). This interpretation would allow a similar assignment of secondary structure as in Figure 3c and suggest that BPPs share structural properties across completely unrelated species.

CD studies on phosvitin have shown that the effects of Ca^{2+} or Mg^{2+} on secondary structure may be different (see previous text). As the insertion of Mg^{2+} determines which polymorph of calcium carbonate is formed in mollusk shells, this property may play an important role in mineralization processes. PfN44, a protein from the Japanese pearl oyster *Pinctada fucata,* reduces the Mg^{2+}-induced formation of aragonite, which leads to calcite crystals with significantly increased content of Mg^{2+} ions.[54] The CD spectra recorded for PfN44 exhibit a minimum at ~210 nm and a negative shoulder between 220 and 230 nm, which would agree with the dispersive curve shape of a spectrum that represents a predominantly unordered protein, even in the absence of bivalent cations (Figure 4b). Upon addition of Ca^{2+} or Mg^{2+}, the minimum at 210 nm becomes less intense. In the presence of Mg^{2+}, this

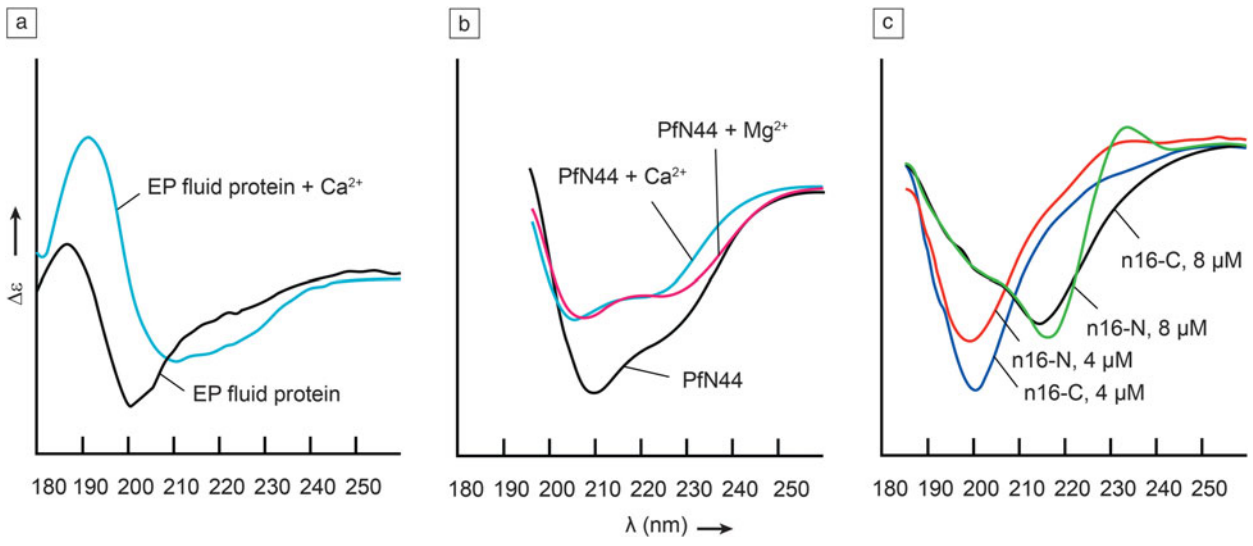


Figure 4. (a) Extrapallial (EP) fluid protein from *Mytilus edulis* in the absence and presence of Ca^{2+}, which induces aggregation. (b) PfN44 in absence or presence of Ca^{2+} or Mg^{2+}. A more pronounced spectral shift indicates a stronger affinity to Mg^{2+} than to Ca^{2+}. (c) Different concentrations of N- and C-terminal peptides from nacre-associated protein n16. Spectral changes at higher concentration indicate associated protein/protein interactions. (a) Adapted with permission from Reference 53. (b) Adapted with permission from Reference 54. (c) Adapted with permission from Reference 61.

https://doi.org/10.1557/mrs.2015.116 Published online by Cambridge University Press

intensity decrease is concomitant with an increase of the shoulder at ~227 nm, which indicates an Mg^{2+}-induced change in secondary structure. This Mg^{2+}-specific effect is possibly crucial for the physiological role of PfN44 in the regulation of calcite/aragonite deposition.

Model peptides

Instead of looking at full-length proteins, numerous studies have investigated peptides that represent domains, which contain amino acid sequence patterns being typical for their capability to control nucleation.[55–59] Some of these peptides show nucleation properties *in vitro.* It is highly probable that their amino acid sequence and the secondary structure these peptides exhibit are the same as in domains that determine the functionality of the corresponding full-length proteins. The C- and N-terminal ends of the nacre-associated oyster shell protein n16 from *Pinctada fucata* contain sequence motifs that are generally associated with Ca^{2+} binding.[60] The 30 amino acid peptides n16-N and n16-C representing these two domains both modulate the morphology of calcium carbonate crystals *in vitro*.[61] A strong negative band at 200 nm in the CD spectra of 4 μM solutions of n16-N and n16-C indicates unordered conformation (Figure 4c). However, at higher concentration (8 μM), a negative band appears at 215 nm, which can be attributed to formation of β-strand conformation. The positive band showing up at 233 nm for n16-N, however, is not associated with a β-sheet. Nevertheless, the significantly different appearance of CD spectra recorded for different peptide concentrations is a clear sign of intermolecular interaction. As aggregation effects have also been observed for BPPs from different organisms, the propensity for protein/protein-assembly may be mediated by amino acid sequences that are typical for Ca^{2+} binding.

Matrix proteins from mammalian physiology

In mammals, calcified tissue is found in bone and teeth. Biomineralization in teeth is particularly interesting, because it contains different kinds of mineralized tissue with different proportions of mineral and organic material. Enamel is the outer layer of a tooth. It contains up to 96% inorganic material, predominantly hydroxylapatite, which renders it the hardest tissue in mammals and gives it its white appearance. Amelogenins are a group of several isoforms of proteins (5–28 kDa) found in the enamel matrix.[62] Knockout mice lacking amelogenin show abnormal formation of enamel, which suggests a potential role of these proteins in mineralization.[63] During enamel production, vesicles containing amelogenins are secreted from the ameloblasts. These are specialized cells that are only present during tooth development. In this process, they interact with potentially charged surfaces, such as phospholipid membranes, proteins, and hydroxylapatite. The layer below the enamel layer is dentin, a porous material that is considerably softer than enamel and contains around 50% of inorganic material. Dentin formation is initiated by odontoplasts. The extracellular matrix contains dentin matrix proteins (DMPs), phosphoproteins that are putatively involved in mineralization.

Effects of temperature

According to its CD spectrum, the recombinant full-length enamel protein porcine amelogenin rP172 adopts a predominantly unordered structure in the presence of Ca^{2+} ions,

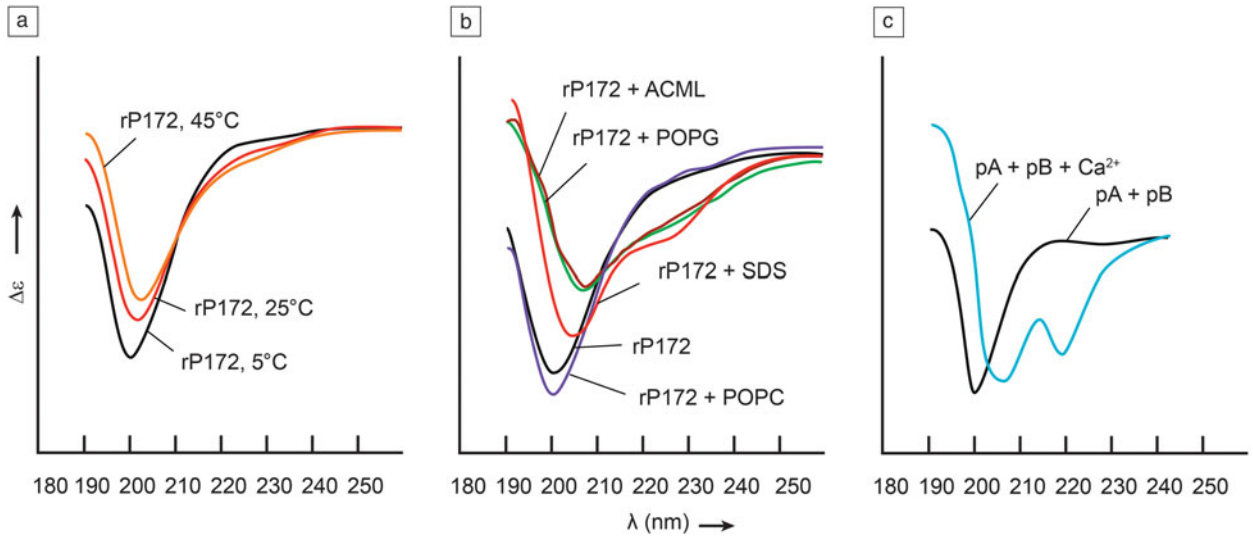


Figure 5. (a) Amelogenin (rP172) at different temperatures in the presence of 5 mM $CaCl_2$. Temperature increase is accompanied by a transition from unordered to β-sheet conformation. (b) rP172 in the presence of lipid vesicles or sodium dodecyl sulfate (SDS) micelles at pH 3.5. Negatively charged lipids (POPG, ACML) invoke aggregation. POPC has no effect, and SDS induces β-sheet. (c) Mixture of peptides pA and pB, representing domains of DMP1, with and without Ca^{2+}. Addition of Ca^{2+} induces assembly and β-sheet. (a) Adapted with permission from Reference 64. (b) rP172 adapted with permission from Reference 68. SDS micelles adapted with permission from Reference 69. (c) Adapted with permission from Reference 74.

https://doi.org/10.1557/mrs.2015.116 Published online by Cambridge University Press

indicated by a strong minimum at 200 nm and a weak positive shoulder at ~220 nm (**Figure 5**a).[64] Increased temperature leads to a shift of the minimum and a decrease of the shoulder. As already discussed for phosvitin, this indicates decreasing content of P_{II}-helix. Interestingly, all CD curves in Figure 5a intersect at one particular point at ~211 nm. The existence of such an isoelliptoic point (referring to constant ellipticity, a synonym for CD intensity) indicates a transition between two states. The linear decrease of the intensity at ~220 nm together with an isoelliptoic point is typical for a temperature-dependent transition from a P_{II}-helix to a β-strand structure.[64–66]

Binding to lipid vesicles

A hallmark of BPPs is the high abundance of acidic residues, suggesting putative effects from protein/cation interactions. However, during the mineralization process, they may also interact with negatively charged surfaces such as lipid membranes, which may have implications for protein structure. This has been described for amelogenin, where the presence of membranes of a particular lipid composition seems to have an impact protein assembly.[67]

For studies on membrane effects, the protein of interest can be mixed with liposomes, which are vesicles composed of lipid bilayers frequently used to mimic a cell membrane in biophysical investigations. Amelogenin rP172 has been tested in the presence of liposomes that consisted either of zwitterionic 1-palmitoyl-2-oleoyl-*sn*-glycero-3-phosphocholine (POPC), negatively charged 1-palmitoyl-2-oleoyl-*sn*-glycero-3-phosphoglycerol (POPG), or a mixture of different lipids chosen to mimic the composition of ameloblast membranes (ameloblast cell membrane-mimicking lipid vesicles, ACML).[68] While the presence of zwitterionic POPC liposomes does not seem to affect the CD spectrum of rP172, the spectra look significantly different in the presence of negatively charged POPG and ACML (Figure 5b). Based on the appearance of the CD spectrum and findings from NMR experiments, which suggest lipid-induced changes of the protein backbone, this was interpreted as a transition to α-helical conformation.[68] However, the CD spectra recorded in presence of POPG and ACML also resemble a dispersive curve shape spectrum of particles that contain a protein in an unordered conformation (Figure 1b). Furthermore, the distribution of hydrodynamic radii determined by dynamic light scattering analyses is slightly different for rP172-POPG and rP172-ACML in favor of larger-sized particles compared to rP172-POPC mixtures.[68] This can be interpreted as a different propensity for protein-protein or protein-lipid assembly for different lipid compositions. Interestingly, while there are significant lipid dependent changes to the CD spectrum at pH 3.5, there are only minor effects observed at pH 8.[68]

Binding to detergent micelles

Sodium dodecyl sulfate (SDS) is a detergent that forms negatively charged micelles. The addition of SDS above its critical micellar concentration to the amelogenin rP172 has led to significant changes in the CD spectrum involving a shift of the characteristic minimum from 200 nm to 208 nm and the formation of a negative shoulder around 220 nm (Figure 5b).[69] These spectral features have been associated with the formation of a

Table I. Biomineralization promoter protein secondary structure.

	Protein/Peptide	Conformation	Perturbation	Invoked Structure	Reference
Avian eggs	Phosvitin	Unordered	pH↓	β-sheet ++++	34, 35
			Mg^{2+}	P_{II}-helix +	43
			Ca^{2+}	β-sheet +	43
			Polycations	Aggregation/β-sheet +++	47
	Ovocleidin-17	Unordered, α-helix	Ca^{2+}	β-sheet +	44
Mollusk shells	EP fluid protein	Unordered	Ca^{2+}	α-helix and/or aggregation (unordered/β-sheet) +	53
	PfN44	Unordered (aggregated), β-sheet	Ca^{2+}	β-sheet +	54
			Mg^{2+}	β-sheet ++	54
	n16-C, n16-N	Unordered	*c*↑	Aggregation	61
Mammalian teeth	Amelogenin (rP172)	Unordered	*T*↑	β-sheet +	64
			Lipids (neg. charge)	α-helix/assembly (pH 3.5)	68
			Lipids (zwitterionic)	Unchanged	68
			SDS	β-sheet ++	69
	DMP1-derived pA + pB	Unordered	Ca^{2+}	Assembly/β-sheet +++	73

Note: According to interpretation of circular dichroism spectra, without and after perturbation by environmental factors.

https://doi.org/10.1557/mrs.2015.116 Published online by Cambridge University Press

β-sheet in other BPPs (see previous text). This agrees with reports that SDS, in spite of its use as a denaturing agent for gel electrophoresis, can sometimes induce local secondary structures in intrinsically disordered proteins.[70] Different from the effects observed for liposomes, the spectral changes observed for the addition of SDS have not been pH-dependent. As the pH-dependent conformational equilibrium in rP172 seems to be nullified by SDS, the interaction with highly charged detergent micelles is probably not viable as a model for the physiological situation.

Model peptides

It has been postulated that the acidic phosphoprotein DMP1 plays a role in calcium binding and mineralization.[71,72] Like other matrix proteins, it contains acidic domains that can possibly interact with calcium.[71] Two short peptides representing such domains (pA and pB) were synthesized and characterized.[73] While neither of these peptides alone has been capable of initiating the crystallization of apatite, a mixture of both induced formation of plate-shaped apatite crystals *in vitro*, which was concomitant with peptide oligomerization.[73] Similar to full-length BPPs, CD spectra of the pA/pB mixture exhibit the characteristic minimum at 200 nm typical of unordered conformation (Figure 5c). In the presence of Ca^{2+}, a minimum around 220 nm indicates the emergence of β-sheet conformation. As β-sheet conformation is generally associated with a higher propensity for self-aggregation,[8] the Ca^{2+}-induced conformational change is possibly driving the self-assembly of pA and pB peptides. It has been hypothesized that self-assembly was a prerequisite for DMP-induced mineralization. This assumption is supported by the fact that CD spectra of the related DMP4 show very similar Ca^{2+}-induced spectral changes as the DMP1-derived acidic domain peptides pA and pB.[74]

Conclusions

In the biomineralization process, controlled nucleation and growth are critical and are the consequence of a complicated interplay involving interactions of BPPs with inorganic salts, proteins, cellular scaffolds, and surfaces. Subtle conformational shifts induced by these interactions may be crucial to stabilize a nucleation-promoting structure. CD spectroscopy is a powerful tool for studying the secondary structure of proteins and has been applied to matrix proteins (or peptides derived thereof) that are involved in biomineralization processes. The presence of particles due to protein interactions may lead to scattering, which can severely complicate the interpretation of CD spectra, in particular if spectral contributions with dispersive line shape interfere with absorptive curves. However, if interpreted carefully, protein aggregation and its associated secondary structure may be identified from the complex overlap patterns of a CD spectrum.

CD analyses of BPPs have shown that they share similar motifs across different species, in most cases indicating unordered structure. This is in agreement with bioinformatics studies that have suggested an unordered secondary structure as an intrinsic property of BPPs.[75] However, taking into account the spectral contributions around 220 nm, it can be concluded that some proteins also contain domains of β-sheet secondary structure. The formation of β-sheet can be invoked by perturbations from the environment, involving pH and/or cation binding (**Table I**). In some cases, these stimuli lead to protein assembly, which putatively plays a role in formation of organic matrices that template mineralization in some contexts. CD spectroscopy therefore can provide the qualitative and quantitative information that is needed to identify the parameters that are necessary to realize this optimal environment for the highly controlled process of biomineralization.

Acknowledgments

This work was funded by a grant from the Helmholtz Zentrum Geesthacht through the Helmholtz Virtual Institute on Multifunctional Biomaterials for Medicine, The Swiss National Foundation-Sinergia Grant (Nr. CRSII3_136179), and the excellence initiative of the German Federal and State Governments Grant EXC 294 (Centre for Biological Signalling Studies) to V. Prasad Shastri and the University of Freiburg.

References

1. S. Boonrungsiman, E. Gentleman, R. Carzaniga, N.D. Evans, D.W. McComb, A.E. Porter, M.M. Stevens, *Proc. Natl. Acad. Sci. U.S.A.* **109**, 14170 (2012).
2. L. Addadi, S. Weiner, *Angew. Chem. Int. Ed.* **31**, 153 (1992).
3. A. George, A. Veis, *Chem. Rev.* **108**, 4670 (2008).
4. N. Kröger, S. Lorenz, E. Brunner, M. Sumper, *Science* **298**, 584 (2002).
5. R. Lakshminarayanan, R.M. Kini, S. Valiyaveettil, *Proc. Natl. Acad. Sci. U.S.A.* **99**, 5155 (2002).
6. W.G. Stetler-Stevenson, A. Veis, *Calcif. Tissue Int.* **40**, 97 (1987).
7. J. Moradian-Oldak, *Matrix Biol.* **20**, 293 (2001).
8. P.N. Cheng, J.D. Pham, J.S. Nowick, *J. Am. Chem. Soc.* **135**, 5477 (2013).
9. R.W. Woody, in *Comprehensive Chiroptical Spectroscopy*, N. Berova, P.L. Polavarapu, K. Nakanishi, R.W. Woody, Eds. (Wiley-VCH, New York, 2012), vol. 2, p. 475.
10. W.C. Johnson, I. Tinoco, *J. Am. Chem. Soc.* **94**, 4389 (1972).
11. S. Brahms, J. Brahms, *J. Mol. Biol.* **138**, 149 (1980).
12. R. Townend, T.F. Kumosinski, S.N. Timasheff, G.D. Fasman, B. Davidson, *Biochem. Biophys. Res. Commun.* **23**, 163 (1966).
13. N. Greenfield, G.D. Fasman, *Biochemistry* **8**, 4108 (1969).
14. G.M. Bonora, C. Toniolo, *Biopolymers* **13**, 1067 (1974).
15. S.N. Timasheff, R. Townend, L. Mescanti, *J. Biol. Chem.* **241**, 1863 (1966).
16. N. Sreerama, R.W. Woody, *Protein Sci.* **12**, 384 (2003).
17. R.W. Woody, *Monatsh. Chem.* **136**, 347 (2005).
18. C. Toniolo, F. Formaggio, R.W. Woody, in *Comprehensive Chiroptical Spectroscopy*, N. Berova, P.L. Polavarapu, K. Nakanishi, R.W. Woody, Eds. (Wiley, Hoboken, 2012), vol. 2, p. 499.
19. J.C. Sutherland,*Comprehensive Chiroptical Spectroscopy*, N. Berova, P.L. Polavarapu, K. Nakanishi, R.W. Woody, Eds. (Wiley, Hoboken, New Jersey, 2012), vol. 1, p. 37.
20. W.C. Johnson, *Annu. Rev. Biophys. Bio.* **17**, 145 (1988).
21. N.J. Greenfield, *Nat. Protoc.* **1**, 2876 (2006).
22. B.M. Bulheller, J.D. Hirst, *Bioinformatics* **25**, 539 (2009).
23. D.W. Urry, J. Krivacic, *Proc. Natl. Acad. Sci. U.S.A.* **65**, 845 (1970).
24. W. Moffitt, A. Moscowitz, *J. Chem. Phys.* **30**, 648 (1959).
25. D.K. Mecham, H.S. Olcott, *J. Am. Chem. Soc.* **71**, 3670 (1949).
26. M. Anton, F. Nau, Y. Nys, *Worlds Poult. Sci. J.* **62**, 429 (2006).
27. X. Zhang, F. Geng, X. Huang, M. Ma, *J. Cryst. Growth* **409**, 44 (2015).
28. K. Onuma, *J. Phys. Chem. B* **109**, 8257 (2005).
29. W.J. Znidarsic, I.W. Chen, V.P. Shastri, *J. Mater. Chem.* **22**, 19562 (2012).
30. E.T. Moran, *Poult. Sci.* **86**, 1043 (2007).
31. M.T. Hincke, C.P.W. Tsang, M. Courtney, V. Hill, R. Narbaitz, *Calcif. Tissue Int.* **56**, 578 (1995).

https://doi.org/10.1557/mrs.2015.116 Published online by Cambridge University Press

32. S.E. Allerton, G.E. Perlmann, *J. Biol. Chem.* **240**, 3892 (1965).
33. V. Giancotti, F. Quadrifoglio, V. Crescenzi, *Eur. J. Biochem.* **35**, 78 (1973).
34. G. Taborsky, *J. Biol. Chem.* **243**, 6014 (1968).
35. S.N. Timasheff, R. Townend, G.E. Perlmann, *J. Biol. Chem.* **242**, 2290 (1967).
36. F. Rabanal, M.D. Ludevid, M. Pons, E. Giralt, *Biopolymers* **33**, 1019 (1993).
37. P. Wilhelm, B. Lewandowski, N. Trapp, H. Wennemers, *J. Am. Chem. Soc.* **136**, 15829 (2014).
38. M.L. Tiffany, S. Krimm, *Biopolymers* **6**, 1379 (1968).
39. Z.S. Shi, R.W. Woody, N.R. Kallenbach, *Adv. Protein Chem.* **62**, 163 (2002).
40. E.R. Blout, M. Idelson, *J. Am. Chem. Soc.* **78**, 497 (1956).
41. K. Grizzuti, G.E. Perlmann, *J. Biol. Chem.* **245**, 2573 (1970).
42. G. Taborsky, *Biochemistry* **2**, 266 (1963).
43. K. Grizzuti, G.E. Perlmann, *Biochemistry* **12**, 4399 (1973).
44. R. Lakshminarayanan, J.S. Joseph, R.M. Kini, S. Valiyaveettil, *Biomacromolecules* **6**, 741 (2005).
45. J.P. Reyes-Grajeda, D. Jáuregui-Zúñiga, A. Rodríguez-Romero, A. Hernández-Santoyo, V.M. Bolanos-Garcia, A. Moreno, *Protein Pept. Lett.* **9**, 253 (2002).
46. D.R. Lide Ed., *CRC Handbook of Chemistry and Physics*, 85th ed. (CRC Press, Boca Raton, 2004).
47. G.E. Perlmann, K. Grizzuti, *Biochemistry* **10**, 4168 (1971).
48. G. Falini, S. Albeck, S. Weiner, L. Addadi, *Science* **271**, 67 (1996).
49. S. Raz, S. Weiner, L. Addadi, *Adv. Mater.* **12**, 38 (2000).
50. S. Weiner, *Biochemistry* **22**, 4139 (1983).
51. E.M. Greenfield, D.C. Wilson, M.A. Crenshaw, *Am. Zool.* **24**, 925 (1984).
52. B.A. Halloran, J.E. Donachy, *Comp. Biochem. Physiol. B: Comp. Biochem.* **111**, 221 (1995).
53. S.J. Hattan, T.M. Laue, N.D. Chasteen, *J. Biol. Chem.* **276**, 4461 (2001).
54. C. Pan, D. Fang, G.R. Xu, J. Liang, G.Y. Zhang, H.Z. Wang, L.P. Xie, R.Q. Zhang, *J. Biol. Chem.* **289**, 2776 (2014).
55. B.A. Wustman, D.E. Morse, J.S. Evans, *Langmuir* **18**, 9901 (2002).
56. M. Michenfelder, G. Fu, C. Lawrence, J.C. Weaver, B.A. Wustman, L. Taranto, J.S. Evans, D.E. Morsel, *Biopolymers* **70**, 522 (2003).
57. S. Hosseini, H. Naderi-Manesh, D. Mountassif, M. Cerruti, H. Vali, S. Faghihi, *J. Biol. Chem.* **288**, 7885 (2013).
58. F.F. Amos, M. Ndao, J.S. Evans, *Biomacromolecules* **10**, 3298 (2009).
59. P.K. Ajikumar, R. Lakshminarayanan, B.T. Ong, S. Valiyaveettil, R.M. Kini, *Biomacromolecules* **4**, 1321 (2003).
60. T. Samata, N. Hayashi, M. Kono, K. Hasegawa, C. Horita, S. Akera, *FEBS Lett.* **462**, 225 (1999).
61. I.W. Kim, E. DiMasi, J.S. Evans, *Cryst. Growth Des.* **4**, 1113 (2004).
62. A.G. Fincham, J. Moradian-Oldak, J.P. Simmer, *J. Struct. Biol.* **126**, 270 (1999).
63. C.W. Gibson, Z.A. Yuan, B. Hall, G. Longenecker, E.H. Chen, T. Thyagarajan, T. Sreenath, J.T. Wright, S. Decker, R. Piddington, G. Harrison, A.B. Kulkarni, *J. Biol. Chem.* **276**, 31871 (2001).
64. R. Lakshminarayanan, I. Yoon, B.G. Hegde, D.M. Fan, C. Du, J. Moradian-Oldak, *Proteins* **76**, 560 (2009).
65. Z.S. Shi, C.A. Olson, G.D. Rose, R.L. Baldwin, N.R. Kallenbach, *Proc. Natl. Acad. Sci. U.S.A.* **99**, 9190 (2002).
66. J. Makowska, S. Rodziewicz-Motowidlo, K. Baginska, J.A. Vila, A. Liwo, L. Chmurzynski, H.A. Scheraga, *Proc. Natl. Acad. Sci. U.S.A.* **103**, 1744 (2006).
67. C.L. Chen, K.M. Bromley, J. Moradian-Oldak, J.J. De Yoreo, *J. Am. Chem. Soc.* **133**, 17406 (2011).
68. S.B. Lokappa, K.B. Chandrababu, K. Dutta, I. Perovic, J.S. Evans, J. Moradian-Oldak, *Biopolymers* **103**, 96 (2015).
69. K.B. Chandrababu, K. Dutta, S.B. Lokappa, M. Ndao, J.S. Evans, J. Moradian-Oldak, *Biopolymers* **101**, 525 (2014).
70. D. Otzen, *Biochim. Biophys. Acta* **1814**, 562 (2011).
71. A. George, B. Sabsay, P.A.L. Simonian, A. Veis, *J. Biol. Chem.* **268**, 12624 (1993).
72. A. George, R. Silberstein, A. Veis, *Connect. Tissue Res.* **32**, 389 (1995).
73. G. He, T. Dahl, A. Veis, A. George, *Nat. Mater.* **2**, 552 (2003).
74. J.J. Hao, K. Narayanan, T. Muni, A. Ramachandran, A. George, *J. Biol. Chem.* **282**, 15357 (2007).
75. L. Kalmar, D. Homola, G. Varga, P. Tompa, *Bone* **51**, 528 (2012). □

THE 2015 MRS SPRING MEETING ON DEMAND

MRS OnDemand®

NEW CONTENT NOW AVAILABLE!

The 2015 MRS Spring Meeting was one of our best yet, and now, with MRS OnDemand, you can view selected talks and lectures from the Meeting, complete with presentation materials, from the comfort of your home or office, or on the go!

▶ FEATURED EVENTS

Fred Kavli Distinguished Lectureship in Nanoscience
Hongyou Fan, Sandia National Laboratories and The University of New Mexico
Nanomaterials under Stress—A New Opportunity for Nanomaterials Synthesis and Engineering

Symposium X—Frontiers of Materials Research
Alexandra Navrotsky,
University of California, Davis
Energetics at the Nanoscale—Impacts for Geochemistry, the Environment and Materials

Lionel Vayssieres, International Research Center for Renewable Energy
Advanced Low Cost Energy Materials from Aqueous Solutions

Daniël Vanmaekelbergh,
Debye Institute for Nanomaterials Science, University of Utrecht
Colloidal Nanocrystals: From Individual Quantum Objects to Building Blocks for Honeycomb Semi-conductors Hosting Dirac Carriers

▶ TUTORIAL SESSIONS

Tutorial P
Nanogenerators and Piezotronics—From Working Principles to Applications

Tutorial Y
Overview of Phase-Change Materials, Their Physics and Applications

Tutorial CC
Reliability and Materials Issues of Semiconductor Optical and Electron Devices and Materials

Tutorial OO
Introduction to Metal-Assisted Chemical Etching—Chemistry and Applications

Tutorial WW
Measure Ultrafast Dynamics—How and Why

▶ SELECT TALKS FROM 12 TECHNICAL SESSIONS

▶ AWARDS OF THE MATERIALS RESEARCH SOCIETY

Mid-Career Researcher Award
Seth R. Marder,
Georgia Institute of Technology
The Design of Organic Molecules and Materials for Nonlinear Optical Applications

Innovation in Materials Characterization Award
John M. Carpenter,
Argonne National Laboratory
History, Development and Applications of Neutron Sources

Outstanding Young Investigator Award
Karena W. Chapman,
Argonne National Laboratory
Accelerating the Development of Energy Materials Through Advanced X-ray Tools

It's YOUR MRS, YOUR WAY | www.mrs.org/on-demand

https://doi.org/10.1557/mrs.2015.116 Published online by Cambridge University Press